Searching for unique neural descriptors of primary colours in EEG signals: a classification study

Sara L. Ludvigsen*, Emma H. Buøen *, Andres Soler, and Marta Molinas

Norwegian University of Science and Technology (NTNU)
Department of Engineering Cybernetics
{sarall, emmahb}@stud.ntnu.no, {andres.f.soler.guevara, marta.molinas}@ntnu.no

Abstract. Identifying unique descriptors for primary colours in EEG signals will open the way to Brain-Computer Interface (BCI) systems that can control devices by exposure to primary colours. This study is aimed to identify such unique descriptors in visual evoked potentials (VEPs) elicited in response to the exposure to primary colours (RGB: red, green, and blue) from 31 subjects. For that, we first created a classification method with integrated transfer learning that can be suitable for an online setting. The method classified between the three RGB classes for each subject, and the obtained average accuracy over 23 subjects was 74.48%. 14 out of 23 subjects were above the average level and the maximum accuracy was 93.42%. When cross-session transfer learning was evaluated, 86% of the subjects tested showed an average variation of 5.0% in the accuracy comparing with the source set.

Keywords: RGB colours · Riemannian classifier · Transfer learning

1 Introduction

Electroencephalography (EEG) signals are obtained from electrodes placed on the scalp recording the macroscopic neural activity. It is a non-intrusive method for recording brain signals, and in BCI systems it can be used by individuals with extreme motor disabilities to manipulate their surroundings. Colour recognition is a novel approach in this area, but has the advantage of being easily applied to control the surroundings. A smart home using colour cues to turn on and off light, open doors, etc. is an example of how to provide more freedom for individuals in their everyday life. Classifying the neural activity evoked by the RGB colour exposure can be enabled by identifying the key features that represent the evoked activity, however, they are often hidden in noise that can come from external sources (artifacts) and the background brain activity. Previous attempts have been made for RGB colour recognition. In [4], the authors identified the EEG signatures produced by the visual exposure to RGB colours. They observed that the difference in frequency response is a good classification

* Equal contribution

signature. In [10] the intrinsic mode functions (IMFs) for Empirical mode decomposition (EMD) were used to identify features in the brain signals that describe the colour activity. The IMFs were used as input to classifiers such as Random Forest (RF) and Naive Bayes. Convolutional Neural Networks (CNNs) were also tried, but not with IMFs as input. Colour vs. none-colour was classified with an accuracy of up to 99% using EMD. The maximum accuracy obtained classifying between RGB colours was 63%, and the maximum average accuracy of 46% using CNNs. A similar attempt was conducted in [9] characterising the signals using discrete wavelet transform and EMD separately. The goal was to classify idle state versus colour exposure. Support vector machine (SVM) and RF were used as classifiers. The most consistent result was obtained using EMD-based features, classifying with an 92.3% accuracy. Another experiment was presented in [5], where a headband with 4 EEG dry electrodes (AF7, AF8, TP9, TP10) was used on eight subjects. The EEG signals were transformed using Morlet transformation and forward feature selection. It achieved an average accuracy of 72.0%, and the highest accuracy of 80.6% when classifying between the RGB colours with a RF classifier.

The scope of this work is to present a method that can be used in an online setting. The focus was therefore to find a methodology that is both fast and accurate in classifying among the RGB colours. EMD and Independent Component Analysis are time consuming operations, and were therefore not evaluated. The decision to use a Morlet wavelet to transform the data was made based on the analysis in Section 2.4. This technique was found advantageous to extract the peaks of several frequencies in the range 2-23 Hz as features. Recording EEG data requires expertise and time. If transfer learning is successful, it allows the reuse of data from previous recordings. Transfer learning across sessions was tested, it was done based on the Riemannian geometry classifiers that have been found suitable for transfer learning [6].

2 Materials and Methods

2.1 Data recording and protocol

The data used in this paper was recorded at the Aalto NeuroImaging facility at Aalto University (Finland). It was recorded using wet EEG electrodes in a high-end 3-layered magnetically shielded room. MEG measurements were recorded simultaneously, but not used in the results presented in this work. 64 electrodes were located on the head, four of which were EOG channels. Two of the EOG channels were placed on the front part of the head, one bipolar EOG channel was placed on the forehead, and below the left eye. The rest of the 60 channels were EEG channels located across the scalp. The placement was done using the international 10/10 system using a 64-channel cap from ANTNeuro, in `https://www.ant-neuro.com/products/waveguard/electrode-layouts` the 64 channel cap layout can be found. For all electrodes, the impedance was kept below 5k Ohm before recording. The subjects were placed in front of a screen that altered between presenting a RGB colour and a grey screen. The RGB colours were presented in a randomised order for 1.3 seconds each, and the grey screen was

presented in a varying length of time to prevent adaptation of the brain. For each subject, at least 140 epochs of each colour were recorded. The subject also had three breaks during the recording, lasting one minute each. All the colours were presented in full-screen mode, and only during grey colour was a cross presented in the middle to keep the eyes of the subjects focused in the same area. Additionally, the subjects were asked to avoid blinking in the colours and try to blink only during grey.

2.2 Dataset

In total, 31 subjects were recorded. For the first recording of subjects 1-18 and subject 26, two of the occipital channels, Oz and O2, were flat. Therefore a second session with all the channels registering was recorded for these participants. The second session was no later than a week after the first session. The remaining 12 subjects participated only in one session. The following requirements were defined to include the subject in the dataset for classification.

1. None of the channels placed over the visual cortex is flat.
2. The subject had a correct behaviour during recording (e.g. looked at the screen, and kept its eyes open)
3. After pre-processing the data (see section 2.3), and removing bad epochs, at least 60 epochs of each colour remains.

This resulted in the dataset consisting of 23 subjects in Table 1. 10-Fold cross-validation was used when calculating classification accuracy. For each subject, 90% of the epochs were used for training, and 10% for testing.

2.3 Data pre-processing

The data was filtered between 0.1 - 40Hz using a band-pass filter, the baseline for each epoch was chosen to be from -100 to 0ms before stimuli were presented, and the data was re-referenced to the common average over all channels. All epochs containing a signal with an amplitude larger than 120μV in the EEG channels and 150μV in the EOG channels were rejected as bad epochs in order to remove artifacts such as blinks and muscular movement from the dataset. Additionally, the subjects were manually inspected for bad channels that were removed if found. The absolute value of the sample with the lowest value in an epoch was added to all samples in the epoch in order to shift the epoch above zero. If the lowest value was positive, it was subtracted from all samples in the epoch. As a final part of the pre-processing, the epochs were cropped to only contain the data between 50 and 450 ms after stimuli for feature extraction. All parameters used in pre-processing are listed in Table 2

2.4 Analysis of Visual Evoked Potentials

The Visual Evoked Potentials (VEP) were extracted and visually inspected for each participant before shifting the epoch above zero. An example of a VEP is shown in fig. 1 where the plots correspond to the VEP of red colour from subject 2 session 2. Figure 1a shows the evoked response of all channels with corresponding

Table 1: The dataset used in this project

Subject	Session	Red epochs	Green epochs	Blue epochs
02	2	134	135	135
03	2	129	124	120
05	2	83	81	82
06	2	134	137	133
07	2	108	110	102
08	2	119	116	115
11	2	122	127	123
13	2	132	129	131
14	2	128	126	126
15	2	103	108	101
16	2	118	126	129
18	2	140	139	139
19	1	114	96	94
20	1	135	137	136
21	1	76	66	69
23	1	125	125	120
24	1	106	113	106
25	1	116	104	108
26	2	120	119	127
28	1	136	136	133
29	1	120	121	117
30	1	117	118	115
31	1	139	135	133

topological-plots for the peaks at 82, 122, and 212ms. It can be seen that there are positive peaks in the nearest channels to the visual cortex, as well as negative peaks in the frontal channels. The strongest peaks were found in the channels at the occipital and parietal regions. This strong activation in those regions was seen for most colours in most subjects. It was, therefore, decided to only use channels P7, PO7, O1, POz, Oz, PO8, P8, and O2 when classifying. Figure 1b presents the VEPs of channel Oz of red colour. The black line represents the evoked of all red epochs, and the image above is the power plot of the activity evoked by red stimuli. There is an identifiable trend for the first 300ms of the signals, where the peaks were found consistent throughout all epochs. These time ranges where the peaks are presented, were selected as the time region of interest for extracting features for classification. The features were extracted by transforming the EEG data with a Morlet wavelet of several frequencies, which is further explained in Section 2.5.

2.5 Feature Extraction

Only eight channels were used for feature extraction and classification. The channels are listed in Table 2. The preprocessed data in each channel was decomposed

Table 2: Parameters

Filter	0.1 - 40 Hz
Reject criteria	EEG: 120e-6, EOG: 150e-6
Baseline	-0.1 - 0.0 sec
Crop	0.05 - 0.45 sec
Channels	P7, PO7, O1, POz, Oz, PO8, P8, O2
Frequencies (Hz) used in CWT	2,5,8,11,14,17,20,23
Number of cyclet in morlet wavelet	0.5

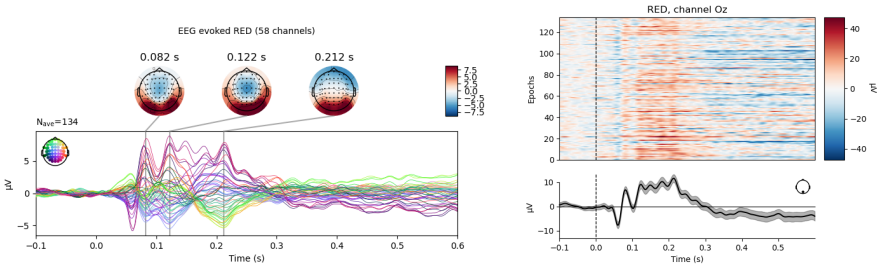

(a) Butterfly plot of the VEPs of red epochs for all channels

(b) VEPs of red epochs on channel Oz

Fig. 1: VEPs of subject 2 session 2

using a continuous wavelet transform (CWT) with a 0.5 cycles Morlet wavelet as the mother wavelet. The correlation between the signal and wavelet was calculated as follows.

$$CWT(a,b) = \frac{1}{|a|^{1/2}} \int_{-\infty}^{\infty} x(t)\psi(\frac{t-b}{a})dt \tag{1}$$

The decomposition was done using a built-in function in the MNE python library [7]. This function calculates the Morlet wavelet as follows.

$$\text{oscillation} = \exp(2j\pi ft) \tag{2} \qquad \text{gaussian envelope} = \exp(-t^2/(2\sigma^2)) \tag{3}$$

$$w(t,f) = \text{oscillation} * \text{gaussian envelope} \tag{4}$$

With the normalisation factor given by

$$A = (\sqrt{0.5}\|w\|)^{\frac{-1}{2}} \tag{5}$$

$$w(t,f) = A\exp(2j\pi ft)\exp(-t^2/(2\sigma^2)) \tag{6}$$

The frequencies used are specified in table 2. Each frequency decomposition in each channel was used as an input for a covariance matrix. Resulting in a 64x64 matrix (eq. (9)). Where the covariance is defined as

$$Cov(X,Y) = E[(X - E[X])(Y - E[Y])] \tag{7} \qquad E[X] = \int_{-\infty}^{\infty} xf(x) \tag{8}$$

$$\mathbf{CVM} = \begin{bmatrix} Cov((ch_1, 2Hz), (ch_1, 2Hz)) & \dots & Cov((ch_1, 2Hz), (ch_8, 23Hz)) \\ Cov((ch_1, 5Hz), (ch_1, 2Hz)) & \dots & Cov((ch_1, 5Hz), (ch_8, 23Hz)) \\ \vdots & \ddots & \vdots \\ Cov((ch_2, 2Hz), (ch_1, 2Hz)) & \dots & Cov((ch_2, 2Hz), (ch_8, 23Hz)) \\ Cov((ch_2, 5Hz), (ch_1, 2Hz)) & \dots & Cov((ch_2, 5Hz), (ch_8, 23Hz)) \\ \vdots & \ddots & \vdots \\ Cov((ch_8, 23Hz), (ch_1, 2Hz)) & \dots & Cov((ch_8, 23Hz), (ch_8, 23Hz)) \end{bmatrix} \tag{9}$$

2.6 Classification

The Minimum Distance to Mean with geodesic filtering (FgMDM) Riemannian classifier [3] was used, due to its robustness to noise [2] and its generalisation capabilities [6].
In [6], the Riemannian distance (δ_G) was defined as the length of the geodesic between two symmetric positive definite matrices, $\mathbf{C}_1$ and $\mathbf{C}_2$, on a Riemannian manifold:

$$\delta_G(\mathbf{C}_1, \mathbf{C}_2) = \left\| \mathrm{Log}(\mathbf{C}_1^{-1/2} \mathbf{C}_2 \mathbf{C}_1^{-1/2}) \right\|_F \tag{10}$$

where $\mathrm{Log}(\cdot)$ is the matrix logarithm. The Riemannian distance is invariant under congruence and invariant under inversion, which means that

$$\delta_G(\mathbf{X}\mathbf{C}_1\mathbf{X}^T, \mathbf{X}\mathbf{C}_2\mathbf{X}^T) = \delta_G(\mathbf{C}_1, \mathbf{C}_2) = \delta_G(\mathbf{C}_1^{-1}, \mathbf{C}_2^{-1}) \tag{11}$$

2.7 Transfer Learning

A challenge in BCI systems is to accurately classify one session data based on data from another session. This is due to the changes in impedance and electrode positioning is likely to vary each time the subject participates in a session.
The EEG signal, $\mathbf{x}(t)$, can be written as a linear combination of the sources of the signal, $\mathbf{s}(t)$:

$$\mathbf{x}(t) = \mathbf{A}\mathbf{s}(t), \tag{12}$$

where $\mathbf{A}$ is the mixing matrix [6]. The mixing matrix $\mathbf{A}$ is dependent upon the impedance and electrode placement. Let the covariance matrices $\mathbf{C}_i = \mathbf{A}\mathbf{S}_i\mathbf{A}^T$ and $\mathbf{C}_j = \mathbf{A}\mathbf{S}_j\mathbf{A}^T$ be representing class i and j, taken from the same session and subject. Let $\mathbf{Q}_i = \tilde{\mathbf{A}}\mathbf{S}_i\tilde{\mathbf{A}}^T$ and $\mathbf{Q}_j = \tilde{\mathbf{A}}\mathbf{S}_j\tilde{\mathbf{A}}^T$ be the covariance matrices taken from another session, with the same subject. Note that $\mathbf{A} \neq \tilde{\mathbf{A}}^T$, because the impedance level and electrode placement varies from session to session. These changes cause a shift in the EEG recording, which makes transfer learning difficult. Due to the congruence invariance property of the Riemannian distance between a pair of symmetric positive definite matrices, the distance between the covariance matrices in the source space are equal for both sessions, as shown in[6]:

$$\delta_G(\mathbf{C}_i, \mathbf{C}_j) = \delta_G(\mathbf{Q}_i, \mathbf{Q}_j) \tag{13}$$

The methods described in this section were implemented and tested in python by using `pyriemann`[1], `scikit-learn`[8] and `mne`[7] libraries.

3 Results

The accuracy of the classification in the results is described as a number between 0 and 1, with 1 as the highest accuracy. The standard deviation of the accuracy is included as "std" in the tables. All results were obtained when classifying between the three classes {Red, Green and Blue}.

3.1 RGB classification

The RGB classification results are presented in table 3, where the results correspond to the subjects in table 1 that fulfilled all the criteria set section 2.2. The average obtained across participants was 74.48% with a standard deviation of 7.5%, where more than 60% of the subjects obtained an accuracy value over the average. Where subject 14 obtained the highest accuracy of 93.42% and subject 31 the lowest with 54.02%. All the subjects obtained scores over the chance level. In addition, table 4 shows the classification accuracy of all subjects with two sessions, where the channels Oz and O2 are excluded, as these channels were flat in session 1 for all subjects. The subjects still had to fulfill criteria 2) and 3) explained in section 2.2.

3.2 Cross-session transfer learning

Cross session transfer learning was evaluated for all subjects in table 4 where both sessions had an accuracy above 60%. The subjects and results for transfer learning are presented in table 5. Average accuracy was computed considering both sessions for the subject in table 4, and the same procedure was done for standard deviation. The column marked "s1 - s2" represents the accuracy obtained when session 1 is used for training, and session 2 is used for testing. Vice versa for the column marked "s2 - s1". "diff" is the difference between the average accuracy of both sessions, and the best performance for transfer learning.

4 Discussion and Conclusion

The results obtained show that using the correlation of the wavelet decomposition with the FgMDM Riemannian classifier for the VEP allowed to separate the colours in most of the subjects. All subjects scored above the chance level 33%, with the accuracy of the lowest performing subject at 54.04%. The average accuracy of 74.48%, which is significantly above the chance level. It clearly states that the features presented can be used to separate the responses of the RGB colours. By analysing the accuracy we can identify that from the subjects that

Table 3: Result of RGB classification of subjects that fulfil all criteria.

Subject	FgMDM	std
s14r2	0.9342	0.056747
s02r2	0.9255	0.050247
s13r2	0.9208	0.021501
s21r1	0.8959	0.05084
s06r2	0.8515	0.050616
s29r1	0.8294	0.065617
s30r1	0.8158	0.0963
s26r2	0.8023	0.088092
s07r2	0.7813	0.108253
s19r1	0.7632	0.050098
s24r1	0.7564	0.085264
s11r2	0.7550	0.092997
s18r2	0.7512	0.09483
s23r1	0.7459	0.109585
s05r2	0.7318	0.084454
s20r1	0.7104	0.077408
s25r1	0.6705	0.110448
s08r2	0.6514	0.064902
s03r2	0.6351	0.07554
s28r1	0.5754	0.067562
s15r2	0.5451	0.096332
s16r2	0.5410	0.065429
s31r1	0.5404	0.061623
Average	**0.7448**	**0.0750**

Table 4: Results of RGB classification of all subjects with two sessions. Not including channel Oz and O2.

Subject	FgMDM	std
s02r1	0.8417	0.0493
s02r2	0.8142	0.0213
s03r1	0.5647	0.0561
s03r2	0.5526	0.0976
s04r1	0.5139	0.0780
s06r1	0.7625	0.0740
s06r2	0.7398	0.0489
s07r1	0.6493	0.1020
s07r2	0.7156	0.0963
s08r1	0.5471	0.0546
s08r2	0.6400	0.0769
s11r1	0.5857	0.0528
s11r2	0.6447	0.0987
s13r1	0.8188	0.0714
s13r2	0.8722	0.0680
s14r1	0.7125	0.0731
s14r2	0.7289	0.1085
s15r1	0.4232	0.0569
s15r2	0.5030	0.0626
s16r1	0.5209	0.0926
s16r2	0.4925	0.0786
s18r1	0.6379	0.0485
s18r2	0.7154	0.0713
s26r1	0.6439	0.0681
s26r2	0.6203	0.0487

scored at approximately 55%[1], the classifier might have been able to recognise at least *one* of the colours, and was guessing between the three classes on the remaining epochs. Similarly, the subjects that scored at approximately 77%[2], the classifier might have been able to recognise *two* of the colours, and guessing at the remaining 33% of the epochs.

The transfer learning test showed that the cross-session model can be used for classifying a different session. Six out of seven subjects obtained a difference lower than 7% when comparing training and testing between sessions with the use of the same session for training and testing. Even with the limited number of subjects with two sessions, we consider that the model is not guessing when classifying a session based on the training on the other. We consider that this aspect should be explored with more subjects in future works. When looking at the confusion matrix in fig. 2a, it can be seen the classifier performed bet-

[1] Accuracy $= 33\% + \frac{1}{3}66\% = 55\%$
[2] Accuracy $= 66\% + \frac{1}{3}33\% = 77\%$

Table 5: Results of cross-section transfer learning.

Subject	Avr. accuracy	Avr. std	s1 - s2	s2 - s1	diff.
02	0.8216	0.0471	0.8119	0.7825	0.0097
06	0,7487	0,0644	0,7253	0,7044	0,0234
07	0.6734	0.1010	0.6000	0.5138	0.0734
13	0.8416	0.0710	0.7679	0.7402	0.0737
14	0.7234	0.09825	0.6474	0.5843	0.0760
18	0.6765	0.0574	0.3373	0.4698	0.2067
26	0.6322	0.0605	0.6066	0.6108	0.0214

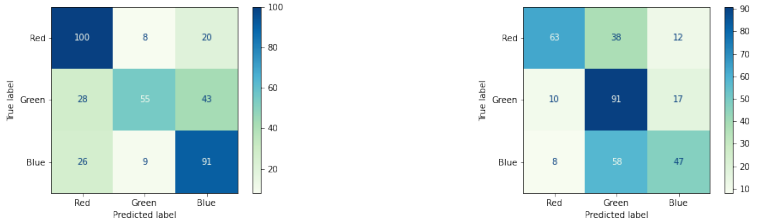

(a) Source = session 1, target = session 2. (b) Source = session 2, target = session 1.

Fig. 2: Session to session classifying for subject 14.

ter at separating red and blue, while in fig. 2b the classifier performed better when separating green. If training on both session 1 and session 2, testing on a session 3 might actually increase performance. Hence, transfer learning using more sessions should be explored as well. It is especially interesting that not any modification of the signal is needed when using a Riemannian FgMDM classifier for testing across-session, making it very convenient for offline modelling and online testing. From the features presented in this paper, the FgMDM classifier does separate between colours using EEG electrodes in a BCI model. It should be easy enough to apply in an online setting, and it also shows promising for applying cross-session transfer learning.

Other classification methods were applied to this dataset as well as the one presented in this paper. An equal feature extraction method in combination with a tangent space Riemannian classifier performed marginally poorer with an average accuracy of 74.43%. Energy, fractal and statistical features were also extracted and used in combination with classifiers such as linear discriminant analysis with shrinkage (LDAs), RF and SVM. Of these, LDAs gave the highest average accuracy of 67.07%.

The accuracy obtained when classifying RGB-colours in this paper are higher than the accuracy obtained in [10] and [5] with an average accuracy of 46% and 70.2% respectively. However, the equipment for recording this dataset used gel based electrodes and impedance was controlled, contrary to [10] and [5], where dry electrodes were used.

Bibliography

[1] Barachant, A., King, J.R.: pyriemann v0.2.2 (Jun 2015). https://doi.org/10.5281/zenodo.18982

[2] Barachant, A., Bonnet, S., Congedo, M., Jutten, C.: Riemannian geometry applied to bci classification. In: Vigneron, V., Zarzoso, V., Moreau, E., Gribonval, R., Vincent, E. (eds.) Latent Variable Analysis and Signal Separation. pp. 629–636. Springer Berlin Heidelberg, Berlin, Heidelberg (2010)

[3] Barachant, A., Bonnet, S., Congedo, M., Jutten, C.: Classification of covariance matrices using a riemannian-based kernel for bci applications. Neurocomputing **112**, 172 – 178 (2013). https://doi.org/https://doi.org/10.1016/j.neucom.2012.12.039, advances in artificial neural networks, machine learning, and computational intelligence

[4] Bjørge, L.E., Emaus, T.: Identification of EEG-based signature produced by visual exposure to the primary colours RGB. Ph.D. thesis, NTNU (07 2017)

[5] Chaudhary, M., Mukhopadhyay, S., Litoiu, M., Sergio, L., Adams, M.: Understanding brain dynamics for color perception using wearable eeg headband. Proceedings of 30th Annual International Conference on Computer Science and Software Engineering 2020 (08 2020)

[6] Congedo, M., Barachant, A., Bhatia, R.: Riemannian geometry for EEG-based brain-computer interfaces; a primer and a review. Brain-Computer Interfaces **4**(3), 155–174 (2017). https://doi.org/10.1080/2326263X.2017.1297192

[7] Gramfort, A., Luessi, M., Larson, E., Engemann, D.A., Strohmeier, D., Brodbeck, C., Goj, R., Jas, M., Brooks, T., Parkkonen, L., Hämäläinen, M.S.: MEG and EEG data analysis with MNE-Python. Frontiers in Neuroscience **7**(267), 1–13 (2013). https://doi.org/10.3389/fnins.2013.00267

[8] Pedregosa, F., Varoquaux, G., Gramfort, A., Michel, V., Thirion, B., Grisel, O., Blondel, M., Prettenhofer, P., Weiss, R., Dubourg, V., Vanderplas, J., Passos, A., Cournapeau, D., Brucher, M., Perrot, M., Duchesnay, E.: Scikit-learn: Machine learning in Python. Journal of Machine Learning Research **12**, 2825–2830 (2011)

[9] Torres-García, A., Moctezuma, L., Molinas, M.: Assessing the impact of idle state type on the identification of rgb color exposure for bci (02 2020). https://doi.org/10.5220/0008923101870194

[10] Åsly, S.: Supervised learning for classification of EEG signals evoked by visual exposure to RGB colors. Ph.D. thesis, NTNU (06 2019). https://doi.org/10.13140/RG.2.2.13412.12165